SCIENCE CHINA
Technological Sciences

• Article •

June 2014 Vol.57 No.6: 1175–1182
doi: 10.1007/s11431-014-5548-7

Effects of the radial force on the static contact properties and sealing performance of a radial lip seal

JIA XiaoHong[1*], GUO Fei[1], HUANG Le[1,2], WANG LongKe[3], GAO Zhi[1] & WANG YuMing[1]

[1] *State Key Laboratory of Tribology, Tsinghua University, Beijing 100084, China;*
[2] *Guangzhou Mechanical Engineering Research Institute Co., Ltd., Guangzhou 510700, China;*
[3] *Eaton Corporation, MN55334, USA*

Received October 11, 2013; accepted February 26, 2014; published online May 9, 2014

The radial force is a critical factor to determine the sealing performance of radial lip seals. The effects of radial force produced by garter spring and interference on the static contact properties and sealing performance of a radial lip seal are investigated by numerical simulations and experiments. Finite-element analysis and mixed elastohydrodynamic lubrication simulation are used. Radial force, contact width, temperature in the sealing zone, the reverse pumping rate and friction torque are measured. A critical value of interference for a cost-effectively designed radial lip seal is found. Spring force is required to compensate the decrease of the radial force because of the interference and used as a possible way to obtain intelligent control of sealing performance. The quantitative results gotten in this study could provide guide for the seal design and improvement.

lip seal, radial force, static contact properties, pumping rate, friction torque

Citation: Jia X H, Guo F, Huang L, et al. Effects of the radial force on the static contact properties and sealing performance of a radial lip seal. Sci China Tech Sci, 2014, 57: 1175–1182, doi: 10.1007/s11431-014-5548-7

1 Introduction

Because radial lip seals have many advantages, such as simple and compact construction, mature processing technic, and less friction during actual operation, they are most widely used in modern machinery to prevent leakage of fluid and exclude contamination in bearing and rotating shaft applications. Figure 1(a) shows a typical type of radial lip seals, composing of steel frame, garter spring and elastomeric ring. The common elastomeric materials include nitrile butadiene rubber (NBR), polyurethane (PU), fluoroelastomer (FKM) etc. NBR is selected as the elastomeric material in this study. The compression molding forming means is the main technology used to manufacture the lip seals.

The radial force, which is related to the leakage and wear, plays a vital role in evaluating the success of a radial lip seal. If it is too small to follow vibrations, wear or eccentricity, the seal will leak. If it is too large, the durability could be diminished due to high friction torque and consequently increased wear and the aging of the elastomer ring. The radial force is not a real force vector. It is the integral of the radial linear contact pressure above the shaft circumference. In general, the contact pressure distribution has a triangle-like profile. Maximum pressure and steep increase occur on the oil side and gentle decline on the air side. This asymmetric distribution can produce a net pumping action from the air-side toward the liquid-side of the lip seal to obtain zero leakage [1–5].

Excessive contact pressure has been identified as a critical cause of seal failure. 2D axisymmetric finite element (FE) model [6–9] is often used to calculate contact pressure

*Corresponding author (email: jiaxh@mail.tsinghua.edu.cn)

between seal lip and shaft for the typical type of radial lip seals shown in Figure 1(a). Approximate 50% of the whole radial force is produced by the garter spring, and the other half of the radial force comes from the elastomer deformation due to the interference fit between the elastomer ring and the shaft shown in Figure 1(b). The effects of interference and geometry design variables on the contact properties were discussed [10]. The contact pressures with the spring were compared with those without spring. There are two ways to simulate the garter spring. It could be directly modeled as a cylindrical solid or a ring- shaped body with suitable material property [6,7,9,11]. On the other hand, the spring was not built in the FE mode, and only the force produced by the spring was applied as a point force or a distributed load [8].

The radial force was also studied by experiments [7,9,12]. The resultant radial force and contact width were measured when the seal was mounted on the shaft with or without the garter spring.

The previous investigations have provided much information on the contact properties of radial lip seals. However, although the radial force is known for having a significant effect on the seal performance, the relationship between the radial force and sealing performance such as the reverse pumping rate and friction torque, have not thoroughly studied. The garter spring and interference, which both provide the radial force, are important to determine interference tolerance δ (difference between the sealing lip inner diameter and the shaft diameter), the stiffness and length of the spring when designing and manufacturing a lip seal. Suitable values can not only maintain enough radial force when wear, aging and stress relaxation happen to the elastomer ring, but also keep friction torque as low as possible. Moreover, adjusting the radial force exerted by the spring, which is called the spring force, may possibly be an easy way to control seal performance for the intelligent lip seal. It is necessary to conduct a detailed study about how the garter spring affects the sealing performance.

Therefore, the objective of this study is to investigate the effects of radial force produced by garter spring and interference on the sealing performance of a radial lip seal by numerical simulation and experiment. A FE model is developed. A mixed elastohydrodynamic lubrication (M-EHL) model built by the same authors is used. Different radial forces are obtained by changing spring length. Temperatures in the contact zone under different radial force or rotary speeds are measured. The contact width, reverse pumping rate, and friction torque are obtained from the validated M-EHL model while various radial forces are applied.

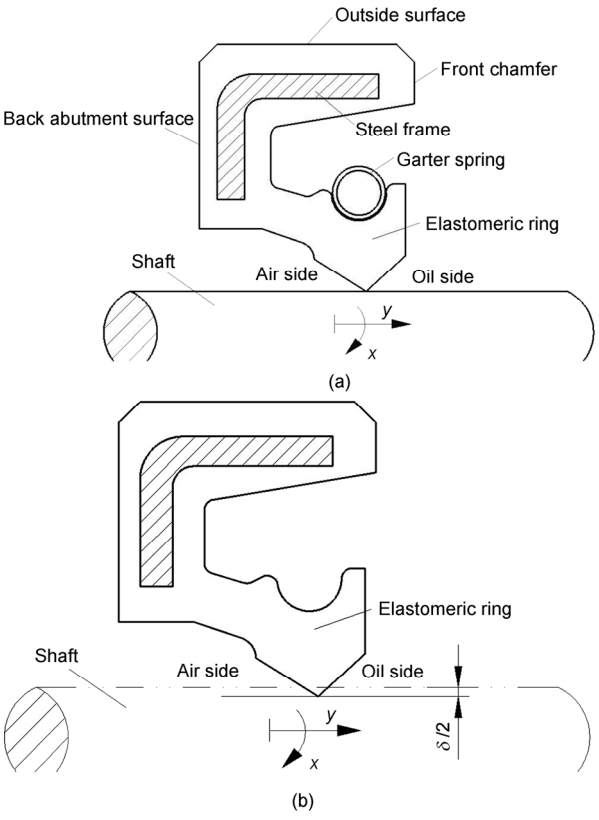

Figure 1 Schematic diagram of (a) a radial lip seal and (b) the interference δ between unsprung seal lip and shaft.

2 Simulation methods

2.1 FE analysis

Due to the axisymmetric structure of the radial lip seal as shown in Figure 1, an axisymmetric 2D model (Figure 2) is developed, utilizing a commercial package, ANSYS. All materials are assumed to be isotropic, homogeneous. Steel frame and shaft are linearly elastic with E=210 GPa and v=0.29. Elastomeric ring is modeled as a Mooney-Rivlin material with C_{10}=0.88702 MPa, C_{01}=−0.41732 MPa, C_{11}= 0.0074 MPa. These constants were curved-fitted from the experiment conducted on the uni-axial compression testing. Contact elements “targe169” and “contac172” are used for simulation contact between the lip and shaft surface. The model is meshed freely, and a mesh refinement near the sealing lip is developed, leading to the mesh size of the model is 4614 elements. The outer circumferential surface and back abutment surface, shown in Figure 1, are fixed in displacement. The oil-side and air-side surfaces of the seal are subjected to the fluid pressure and the atmospheric pressure respectively. Both are 0.1 MPa.

The analysis is performed in two load steps. In the first step, the upper line of the shaft (it stands for the shaft surface in the 2D model) is moved upward to the seal by applying the displacement. This displacement equals to the difference in radius between unsprung seal lip and shaft, half of interference tolerance, as shown in Figure 1(b). As a result, pre-stresses between the contact surfaces are produced. In the second step, the spring force is applied on the

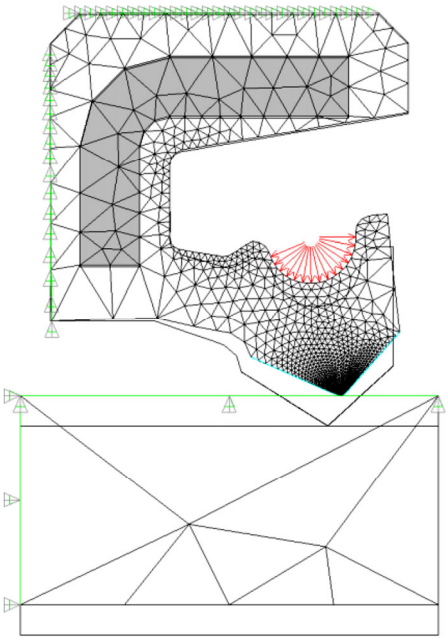

Figure 2 (Color online) Finite element model.

spring groove as a surface pressure. This pressure is calculated based on the groove area and the measurement results of radial force with garter spring and without garter spring using the test plant shown in the Figure 4 (see Section 3.1).

2.2 Numerical analysis using a M-EHL model

Numerical approaches have often been used to study the sealing behavior of the radial lip seal. A mixed elastohydrodynamic lubrication model that was previously constructed by the same authors is used in this study [13]. It is outlined below.

The model consists of a coupled hydrodynamic lubrication analysis, asperity contact analysis, and deformation analysis, with an iterative computational procedure. The fluid mechanics of the lubricant film in the sealing zone is governed by the Reynolds equation. Asperity contact pressure is computed using the Greenwood and Williamson surface contact model (the G-W model). In the deformation analysis, the normal deformation of the lip is calculated to update the film thickness. An influence coefficient method is used by the above FE model.

Since these analyses discussed above are strongly coupled, it is necessary to use an iterative computational procedure, as illustrated in Figure 3. After all the computations are converged, auxiliary calculations are performed for reverse pumping rate and friction torque.

The reverse pumping rate and friction torque predicted by this simulation model are compared with the experiment results measured with the test rig developed by the same authors. The validated simulation model can be used for further calculation of the sealing performance of the radial lip seal under other cases.

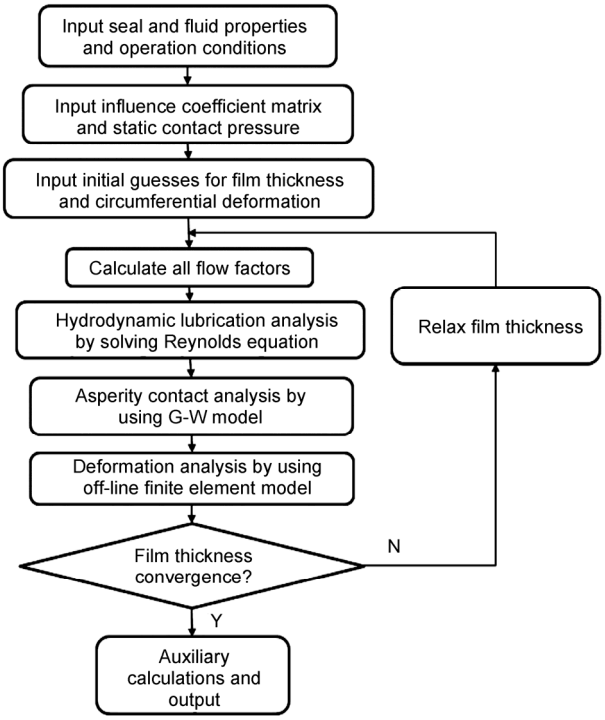

Figure 3 Computational procedure.

3 Experimental study

Several experiments are performed to provide parameters for the simulation or to validate the simulation results.

3.1 Static contact width measurement

Contact width is one of the important indices to assess the static property of lip seals. Figure 4 presents the device set-up to measure the static contact width. It consists of a SLR camera connecting to a computer, a microscope (OLYMPUS SZX12), a transparent sleeve, a two-dimension platform, a powerful light source, and a reflecting mirror which is fixed in the sleeve at 45°. The transparent sleeve has the same diameter as the shaft. After the seal is mounted on the sleeve for 5 h, the contact width can be measured by the

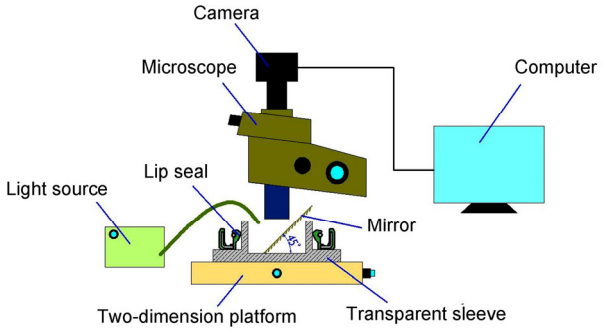

Figure 4 (Color online) Schematic of static contact width measurement.

microscope. In order to eliminate the test error caused by the glass refraction, a grating scale with fixed width 0.15 mm, which is measured by the three coordinate measuring instrument (made by Beijing Tianhong Precision Instrument Technology Co., Ltd, the resolution is 0.5 μm), is aligned with the seal to calibrate the tested length.

3.2 Radial force measurement

Radial force is the integral of the static contact pressure above the shaft circumference, it can be calculated by

$$F_r = \int_0^{\pi D} \int_0^{L_y} P_{sc} \mathrm{d}x\mathrm{d}y, \quad (1)$$

where D and L_y represent shaft diameter and contact width respectively, and P_{sc} represents the static contact pressure.

The radial force is measured to determine the spring force for the FE model and also to validate the general correctness of the FE analysis in predicting the contact behavior. Figure 5 illustrates the schematic diagram of the test plant used in the present study (made by Jiangsu Mingzhu Testing Machinery Company, China). This device, which is newer than DIN3761-9, has a short shaft, split in half lengthwise. One half is rigidly fixed and the other is connected to a force transducer. When the seal is mounted on the shaft, the movable part deflects slightly to trigger the force transducer to measure the radial force.

The measurement is carried out at room temperature. After the seal is mounted for 5 h, the seal is assumed quasi-stationary and the force value can be read. Each seal is measured three times to get average, 120° rotating is made for each measurement.

3.3 Bench test

The bench test is used to provide temperature in the sealing zone for the simulation model and to provide reverse pumping rate and friction torque to validate the numerical simulation results. Figure 6 shows a schematic diagram of the experimental apparatus. The seal is installed reversely, with the original air-side of the seal now exposing to the oil, becoming the oil-side, while the original oil-side has become the air-side. Consequently, the leakage rate measured by this configuration is equivalent to the pumping rate under the normal operating conditions of the radial lip seal. The leaking lubricant oil is collected by an oil-collecting cup and measured using a precision electronic scale with a resolution of 0.01 g (JJ series product, made by G&G Measurement Plant, China). In order to measure the friction torque, a JN338F static torque sensor (made by Beijing Sanjing Creation Science & Technology Group Co., Ltd.) with the resolution of 0.001 N m and measuring range of 5 N m is used. One side of the static torque sensor is connected to the chamber and the other side is fixed to the support seat.

The bench test is carried out under hydraulic oil (ISO 32) lubrication condition. The viscosity of the hydraulic oil is 0.0272 Pa s under the condition of 40°C. The viscosity is an important factor for fluid mechanics. Its decrease makes the film thickness in the sealing zone decrease, resulting in the reverse pumping rate decrease. The viscosity is a function of temperature in the sealing zone which changes with shaft rotation speed and the radial force. As the result, the pumping rate changes, too. A thermal imaging camera ImageIR 8300 (made by InfraTec GmbH Infrarotsensorik Und Messtechnik, Dresden, Germany) is used to measure temperature in the sealing zone, shown in Figure 6.

The seal is assumed working stably when on-line detected friction torque and shaft rotation speed don't change. For each seal with different garter spring, the shaft rotation speed variesin 6 stages, from 500 to 3000 r/min, then to 500 r/min again, this process is treated as a speed change cycle. The average temperature for each speed is calculated by three speed change cycles. According to the viscosity-temperature relationship of the lubricant, viscosity for different radial force and shaft rotation speed can be curve-fitted.

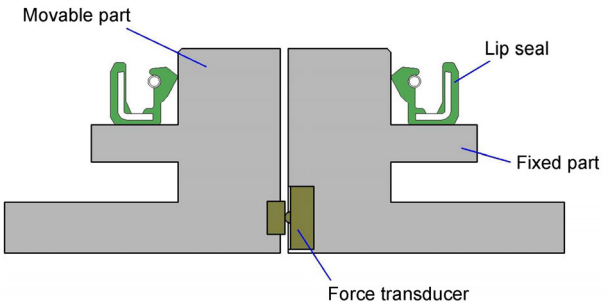

Figure 5 (Color online) Schematic diagram of test plant for measuring the radial force.

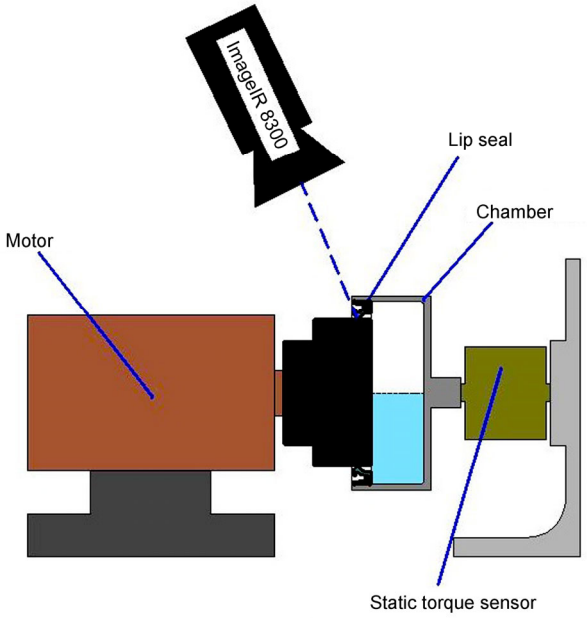

Figure 6 (Color online) Schematic of bench test.

4 Results and discussion

4.1 Validation of FE and M-EHL simulation model

The seal parameter values used in the present study are as follows: diameter of the shaft D=100 mm; cavitation pressure p_{cav}=0, cavitation occurs when the film pressure falls below the catitation pressure of dissolved gases in the lubricant [14]; sealing fluid pressure p_s=0.1 MPa, ambient pressure p_a=0.1 MPa, meaning no pressure difference; lip surface roughness σ=1 μm, asperity autocorrelation length λ_x=1.667 μm and λ_y=5.0 μm, asperity radius R=4 μm. The above four parameters are used to describe the asperities characteristics, which are the best guess at the steady-state configuration of the roughness [14,15]. Friction coefficient f=0.15, obtained from the standard friction test; static undeformed film thickness h_s=1.4 μm, as an initial hypothetical value; fluid density ρ=(857.1–0.0059ω) kg/m^3 and the relationship between fluid viscosity μ and shaft rotation speed ω: μ=[0.02807·exp(ω/2391.5997)+0.00399] Pa s which are obtained from the method of Section 3.3 [16], the unit of ω is r/min. During the FE analysis, the interference of 0.75 mm and surface pressure of 0.012 MPa produced by spring, are applied according to the parameters of the existing lip seal product manufactured by the Guangzhou Mechanical Engineering Research Institute Co., Ltd. The contact width L_y and influence coefficient matrix can be obtained from the FE analysis. The length of solution domain in x direction L_x is set equal to L_y. It should be noted that the parameters of describing the asperities, lip surface roughness, autocorrelation length and asperity radius, are the best assumption under the steady-state configuration of the surface microtopography.

Figure 7 shows the static contact pressure distribution from the FE analysis, without the existence of the lubricant oil film. The distribution curve is typical for a successful lip seal; the maximal pressure at an axial location is closer to the liquid-side of the lip seal than to the air-side. It is also seen that the contact width L_y is about 0.11285 mm. Figure 8 shows the results using the method of Section 3.1. For the fixed width of the grating scale 0.15 mm, it can be obtained from Figure 8(a) that 1 Pixel is equal to 0.8918 μm. Then, from Figure 8(b), it is easy to obtain the experimental contact width, which is equal to 0.117 mm. As a result, the relative error between simulated and experimental value is 3.7%. The radial force can be obtained from eq. (1), the result of the distribution of Figure 7 is 22.82 N. The experimental radial force using the method of Section 3.2 is 22.7 N. The relative error is 0.52%.

The theoretical simulation results and the corresponding experimental results of the pumping rate and friction torque are shown in Figures 9 and 10. Note that these two figures are used only to validate the M-EHL model.

Figure 9 shows the theoretical and experimental change

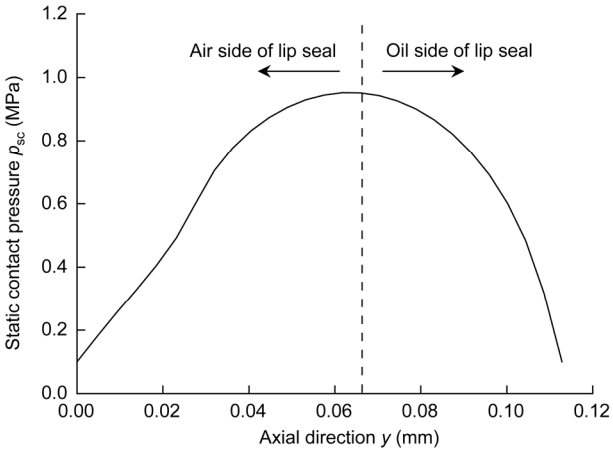

Figure 7 Static contact pressure distribution.

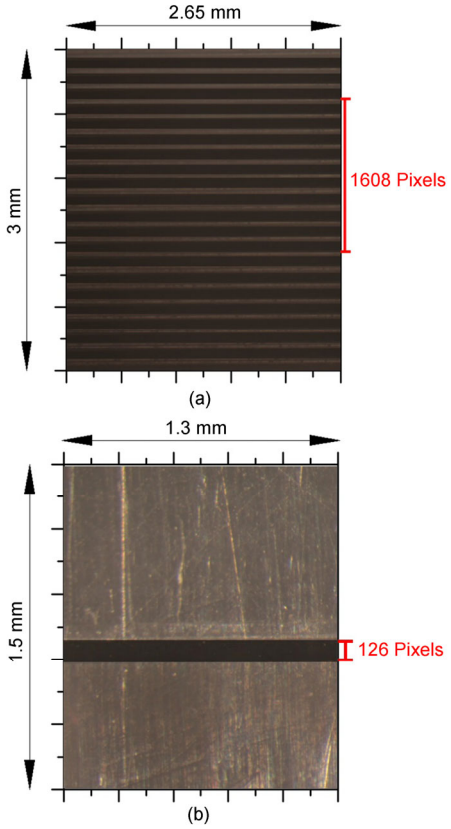

Figure 8 (Color online) Measurement of the contact width.

curves between the reverse pumping rate and rotation speed. It can be seen that the variation trend of the pumping rate changing with speed is almost linear. Note that there is no curve fitting for the simulation results. It is most important to note that there is an excellent agreement between the theoretical and the experimental results.

Figure 10 shows a plot of friction torque changing with rotation speed. From the ref. [13] it can be seen that the friction torque is principally proportional to the product of the viscosity of the lubricant oil and the rotation speed. Un-

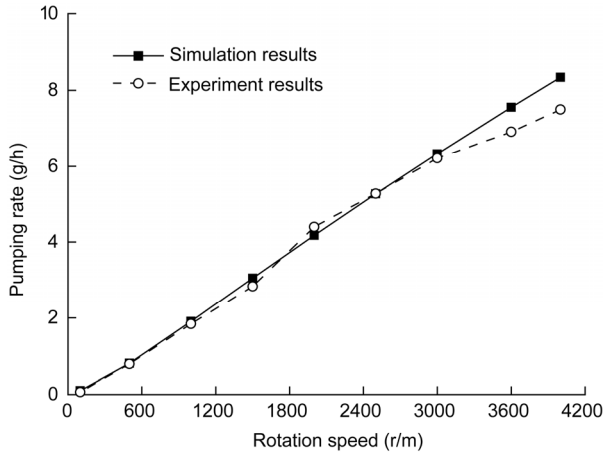

Figure 9 Pumping rate versus rotation speed.

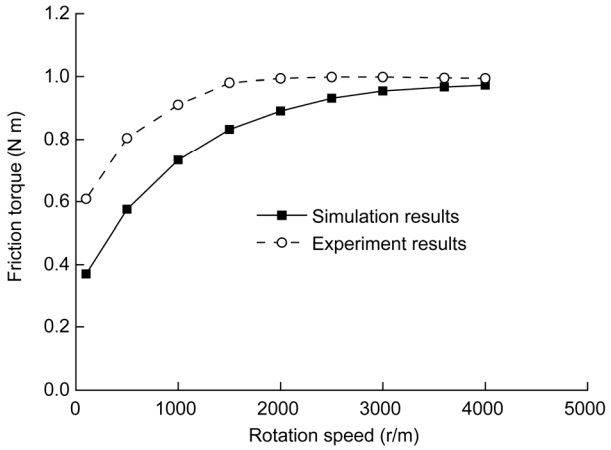

Figure 10 Friction torque versus rotation speed.

der the condition of low speed, the rotation speed has primary impact on the friction torque, so the friction torque increases with rotation speed. However, while the speed increasing, the viscosity of the lubricant oil decreases, so that the friction torque reaches a maximum value at 2000 r/min or so, and then remains almost constant. It is also to note that there is no curve fitting for the simulation results. From the figure, it is also seen that at low speeds the experimental results is larger than the theoretical results, it maybe because the friction coefficient is smaller in the simulation than the actual value. But, the difference is acceptable. Overall, there is a good agreement between the theoretical and the experimental results.

4.2 Comparison of sealing performances produced by interference and spring force

After the above validation, the M-EHL model can now be used to evaluate the reverse pumping rate and friction torque of radial lip seals. Both spring force and interference between shaft and seal ring can produce radial force. Assume that F_s and F_δ represent the radial force produced by spring and interference respectively. Figures 11 and 12 present the simulated reverse pumping rate Q and friction torque T when radial force changes (taking an example when ω=2000 r/min). Here, the radial force is produced by spring force or interference separately. T increases linearly with radial force. The same radical force causes the same T no matter interference or spring force is applied. This means friction torque mainly depends on amplitude of radial force. Meanwhile, F_s also makes Q increase linearly. However, Q becomes stable after a linear rise with F_δ. Normally, higher reverse pumping rate leads to higher friction torque. For a well-designed lip seal, there should be a balance between Q and T. Obviously, it is not cost-effective when F_δ is larger than certain threshold. In this example, this threshold is 14.2 N, corresponding to interference of 0.84 mm along the radius.

4.3 The effects of spring force on static contact properties and sealing performance

During operation of a radial lip seal, the radial force produced by interference decreases with wearing due to relative motion between lip seal and shaft, swelling caused by lubricant oil and stress relaxation resulted from the viscoelasticity of rubber. So, besides the radial force provided from interference, spring force is essential to compensate the decrease of the radial force produced by interference. Moreover, the spring force is a critical factor to determine the life time of a lip seal with given structure and material. Assuming the interference of 0.75 mm, a further discussion is made on the variation of static contact properties and sealing performances of lip seals with spring force.

Figure 13 shows the static contact pressure distributions at different spring forces, under the same interference condition. As one might expect, the maximum contact pressure increases with spring force, and the contact width also increases with spring force, shown in Figure 14. The overall trends of simulated and experimental curves of contact

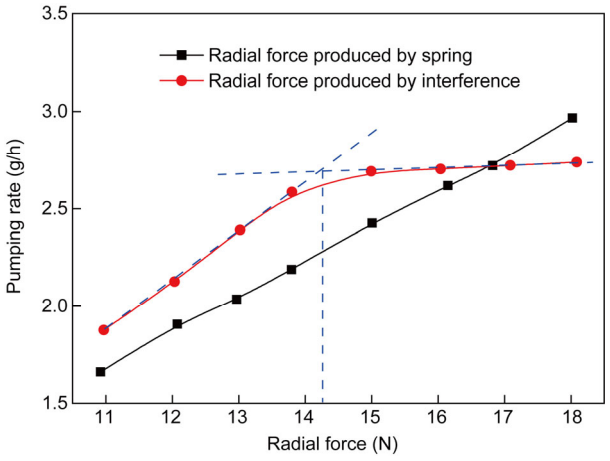

Figure 11 (Color online) Pumping rate versus radial force.

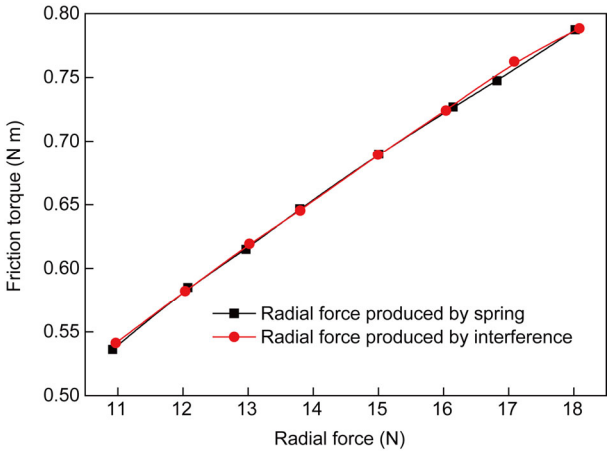

Figure 12 (Color online) Friction torque versus radial force.

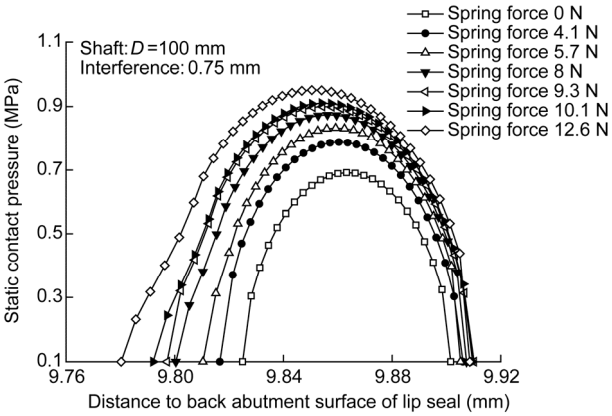

Figure 13 Static contact pressure distributions at different spring forces.

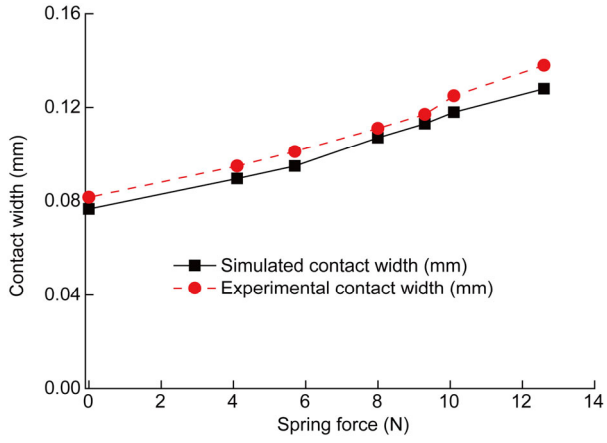

Figure 14 (Color online) Contact width versus spring force.

width are similar. Furthermore, there is excellent agreement between the simulated and experimental radial force, shown in Figure 15. Maybe, the surface of the transparent sleeve, shown in Figure 4, is too smooth, making the adsorption force between the molecules of the sleeve and lip seal increase relative to the surface of the metal shaft, which results in the experimental contact widths are larger than the simulated results, and the differences of both are basically constant.

Figure 16 shows the variation of the temperature of contact area with radial force at the rotation speed of 2000 r/min, with the fitting formula. According to the viscosity-temperature relationship of the lubricant, the relationship between viscosity and radial force can be established. The corresponding viscosity under any radial force can be obtained from the relationship. So, the viscosity need not be obtained through experiment every time. Once the viscosity is obtained, along with the parameters mentioned above, the M-EHL model can be used to predict the pumping rate and friction torque of lip seals. Figures 17 and 18 present the simulated reverse pumping rate Q and friction torque T when spring force changes at the rotation speed of 2000 r/min. Back to the Figure 13, the asymmetry of static contact pressure distribution increases with spring force, and the net reverse pumping of lip seals depends on the asymmetry. So, the pumping rate increases with the spring force. It is obvious that the friction torque also increases with spring force because the whole radial force increases.

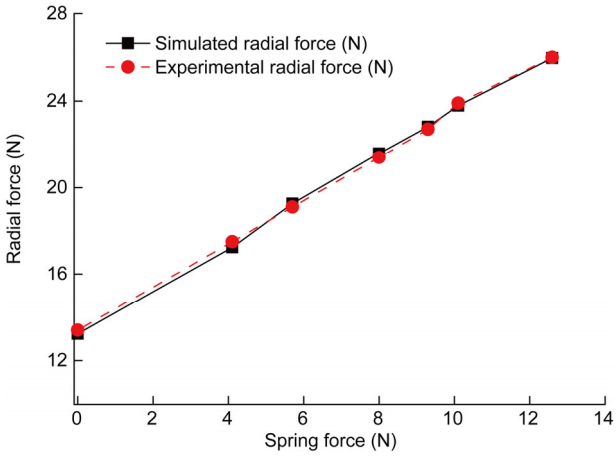

Figure 15 (Color online) Radial force versus spring force.

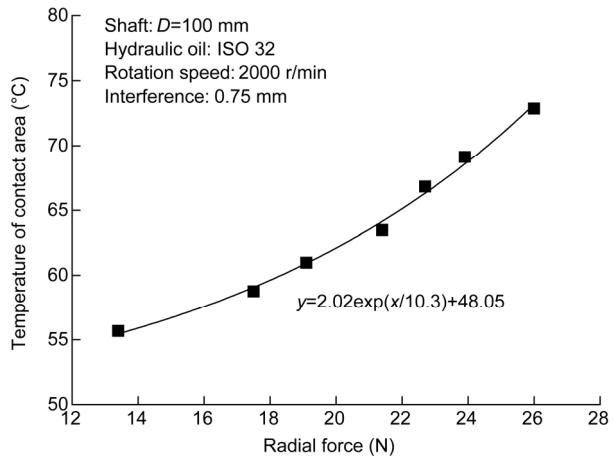

Figure 16 Temperature of contact area versus radial force.

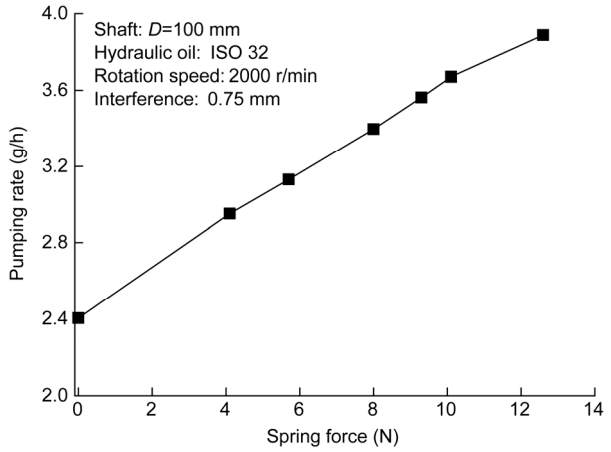

Figure 17 Pumping rate versus spring force.

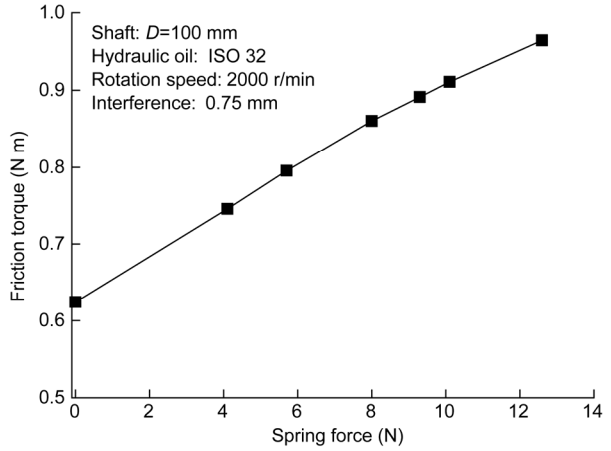

Figure 18 Friction torque versus spring force.

The increase of spring force necessarily improves sealing effect, but it will result in the temperature of contact zone rise, thus accelerating lip seal aging, and the friction torque increase, thus accelerating lip seal wearing, which will decrease the lip seal's service life. However, enough spring force is also essential to compensate the decrease of radial force due to lip wear, lubricant aging and stress relaxation etc. There should be a balance between the sealing performance and lifetime.

5 Conclusions

Finite-element analysis and mixed elastohydrodynamic lubrication simulation were used in this study to investigate how the radial force quantitatively affects the static contact properties and sealing performance. Several types of experiments were also done to validate the simulation results. They show good agreement.

It was found that there is a critical value of interference for a cost-effectively designed radial lip seal. Spring force is necessary to compensate the decrease of the radial force produced by interference and it's a possible way to obtain intelligent control of sealing performance. The quantitative results obtained in this study could provide guide for the seal design and improvement.

This work was supported by the National Natural Science Foundation of China (Grant No. 51175283), the National Science and Technology Major Project of China (Grant No. 2013ZX04010021) and the Ph.D Programs Foundation of Ministry of Education of China (Grant No. 20130002110006)

1 Qian D S. The sealing mechanism and design factors of radial lip seals for crankshafts. Chin Int Combust Engine Eng, 1984, 5: 10–13
2 Kammüller M. Zur Abdichtwirkung von Radial-Wellendichtringen. Dissertation of Doctoral Degree. Stuttgart: Stuttgart Unvi, 1986
3 Müller H K. Concepts of sealing mechanism of rubber lip type rotary shaft seals. In: Proceedings of BHRA 11th International Conference on Fluid Sealing, Cannes, France, 1987
4 Müller H K, Nau B S. Fluid Sealing Technology-Principles and Applications. New York: Marcel Dekker Inc, 1998
5 Stakenborg M J L. On the sealing mechanism of radial lip seals. Tribol Int, 1988, 21: 335–340
6 Kim C K, Shim W J. Analysis of contact force and thermal behavior of lip seals. Tribol Int, 1997, 30: 113–119
7 Lee C Y, Lin C S, Jian R Q, et al. Simulation and experimentation on the contact width and pressure distribution of lip seals. Tibol Int, 2006, 39: 915–920
8 Salant R F, Flaherty A L. Elastohydrodynamic analysi of reverse pumping in rotary lip seals with microundulations. ASME J Tribol, 1994, 116: 56–62
9 Jennewein B, Frölich D. Simulation of the radial force of radial shaft seal rings at different temperatures and aging conditions. In: Proceedings of 17th International Sealing Conference, Stuttgart, Germany, 2012
10 Obayashi S. Analysis to reduce the sliding friction of power steering rod seals. SAE Trans, 1999, 107: 1063–1066
11 Plath S, Meyer S, Wollesen V M. Friction torque of a rotary shaft lip type seal-a comparison between test results and finite element simulation. Mechanika, 2005, 4: 55–59
12 Keitzel H, Meyer S, Wollesen V. Enhancement of the measurement of the radial force of radial lip seals in accordance with DIN 3761, PART 9 by consideration of the influence of temperature and lubrication medium as basis for the modelling. LŽŪU ŽŪI instituto ir LŽŪ Universiteto mokalo darbai, 2005, 37: 146–459
13 Guo F, Jia X H, Salant R F, et al. A mixed lubrication model of a rotary lip seal using flow factors. Tribol Int, 2013, 57: 195–201
14 Harp S R. A computational method for evaluating cavitating flow between rough surfaces. Dissertation of Doctoral Degree. Georgia: Georgia Institute Tech, 2000
15 Guo F, Jia X H, Huang L, et al. The effect of aging during storage on the performance of a radial lip seal. Polym Degrad Stab, 2013, 98: 2193–2200
16 Jia X H, Jung S, Haas W, et al. Numerical simulation and experimental study of shaft pumping by laser structured shafts with rotary lip seal. Tribol Int, 2011, 44: 651–659